GLOBAL BIOGEOCHEMICAL CYCLES, VOL. 11, NO. 4, PAGES 599-612, DECEMBER 1997

Role of dissolved organic matter in the marine biogeochemical cycle: Studies using an ocean biogeochemical general circulation model

Yasuhiro Yamanaka[1]

Center for Climate System Research, University of Tokyo, Tokyo, Japan

Eiichi Tajika

Geological Institute, School of Science, University of Tokyo, Tokyo, Japan

Abstract. A biogeochemical general circulation model which includes production and consumption processes of dissolved organic matter (DOM) is developed. The semilabile and the refractory DOM are taken into account. The vertical distribution of the dissolved organic carbon (DOC) concentration and the $\Delta^{14}C$ value obtained in our model compares well with the recent observations. It is found that the double DOC maximum zone (DDMZ) extends in the east-west direction in the equatorial Pacific. Case studies, which change the decay time and production ratio constant, show that the horizontal distribution of DOC in the surface layer can be reproduced only when the decay time of the semilabile DOM is about half a year. The semilabile DOM exists only above a depth of 400 m, and its vertical and horizontal transport plays an important role in the marine biogeochemical cycle in the surface layer. However, below that depth, only the inert refractory DOM exists, and the role of the refractory DOM in the biogeochemical cycle is not important. The global export production due to the particulate organic matter (POM) and DOM at a depth of 100 m is estimated to be about 8 Gt C/yr and about 3 Gt C/yr, respectively. The vertical transport below 400 m is due almost entirely to POM.

1. Introduction

Dissolved organic carbon (DOC) is considered to play an important role in the marine carbon cycle. *Siegenthaler and Sarmiento* [1993] suggest in their review paper that the DOC transport from the surface layer to the intermediate and the deep layer is 6 Gt C/yr, which is larger than the flux of particulate organic carbon (POC). However, the vertical/horizontal distribution of DOC determined by the high-temperature combustion (HTC) method has been reported only for limited areas [e.g., *Tanoue*, 1993], and its global distribution and flux are not well known.

DOC concentrations determined by the HTC method of *Suzuki et al.* [1985] and *Sugimura and Suzuki* [1988] were extraordinarily high compared to the determinations by previous methods, such as the wet chemical oxidation method. However, their reports were withdrawn by *Suzuki* [1993]. Recent observations show that the DOC concentrations determined by the HTC method are still higher [*Tanoue*, 1992, 1993] or almost the same [*Sharp et al.*, 1995] as those by the wet chemical oxidation method. *Tanoue* [1993] showed that the DOC concentration in the surface water has a spatial variation of about 60 μmol C/kg between the northern North Pacific and the equatorial Pacific. *Peltzer and Hayward* [1996] reported that the total organic carbon concentration in the Pacific surface water along 140°W is 60 μmol C/kg at the equator and 80 μmol C/kg at 10°N and 10°S, but in the deep water it is almost constant at about 36 μmol C/kg. Seasonal variability exists in the surface DOC concentration [*Carlson et al.*, 1994]: DOC accumulates due to the spring bloom, it is partially consumed in summer and autumn, and it is transported under the euphotic layer by convection in winter. The DOC concentration in the deep water is almost constant from the North Atlantic to the Pacific [*Martin and Fitzwater*, 1992]. Comparison of the absolute values of the DOC concentration among various observations is difficult because of errors due to different blank levels

[1]Now at Program in Atmospheric and Oceanic Sciences, Princeton University, Princeton, New Jersey

Paper number 97GB02301.
0886-6236/97/97GB-02301$12.00

among various laboratories [*Toggweiler and Orr*, 1993; *Tanoue*, 1993]. However, the attempts to correct for the instrument blank have led to more accurate measurement of DOC [*Sharp*, 1993]. $\Delta^{14}C$ values of DOC, $(\Delta^{14}C)_{DOC}$, in the deep North Atlantic and the deep North Pacific are about $-400‰$ and $-520‰$, respectively [*Bauer et al.*, 1992]. The horizontal contrast of $(\Delta^{14}C)_{DOC}$ between the North Atlantic and the North Pacific is about the same as that of $\Delta^{14}C$ of the dissolved inorganic carbon (DIC). Those observed features suggested that DOC is transported along with the deep water, with most being conserved.

Previous studies using biogeochemical general circulation models (BGCM) show that the observed distributions of chemical tracers such as phosphate are reproduced only when DOM is included in the models [*Bacastow and Maier-Reimer*, 1991; *Najjar et al.*, 1992]. The calculated DOC concentration, however, seems to be unrealistically higher than that recently observed, because the DOC concentration is based on the observation of *Sugimura and Suzuki* [1988]. *Anderson and Sarmiento* [1995] showed that the problem of nutrient trapping shown by *Najjar et al.* [1992] is resolved, even if the DOM concentration is assumed to be much lower than that of *Najjar et al.* [1992]. Decay time of their DOM, whose global production rate is about 10 Gt C/yr, is longer than 50 years, being too long to explain the seasonal variation of DOC. In a recent version of their model, a DOM decay time of 11.4 years is obtained using as the average DOM concentration in the upper ocean, whose volume is 12% of the total ocean volume, a value 35 μmol/kg higher than that in the deep ocean (R. Murnane, personal communication, 1997). However, recently, *Yamanaka and Tajika* [1996] (hereafter YT) suggested that the observed phosphate distribution can be reproduced in a BGCM even when only POM is considered. *Matear and Holloway* [1995] also suggested that the result of the model with only POM transport is consistent with the observed phosphate distribution when a small modification is made on the circulation field of the Hamburg large-scale geostrophic (LSG) model. *Maier-Reimer* [1993] improved their model without DOM processes, and the calculated distributions of tracers have better resemblance with the observation. Therefore the influence of DOM in determining the phosphate distribution might be small. To clarify the role and behavior of DOC in the oceanic carbon cycle, we need new modeling of DOM based on the recent observations.

From the viewpoint of the role of DOM in the biogeochemical cycles, DOM is conceptually categorized into three components by timescale, as the composition of DOM is not well known. *Kirchman et al.* [1993] reported that models dealing with DOM need to consider at least the following three pools of DOC: (1) a labile pool with turnover time of days or less, (2) a semilabile (semirefractory) pool with seasonal timescale, and (3) a refractory pool with extremely long turnover time (centuries or longer). Although the labile DOM plays an important role in ecosystem modeling [e.g., *Fasham et al.*, 1990; *Kawamiya et al.*, 1994], we estimate its concentration to be much smaller than 10 μmol C/kg. Its flux may not directly affect the global biogeochemical cycle. Therefore we study the global biogeochemical cycle by using a model in which the semilabile DOM and the refractory DOM are taken into account. In this study, the semilabile and the refractory DOM(DOC) will be abbreviated to SDOM(SDOC) and RDOM(RDOC), respectively. Since observation cannot distinguish SDOC from RDOC, we will not directly compare individual features of SDOC and RDOC obtained in the model with the observation. However, we will explain many observed features of total DOC, the sum of SDOC and RDOC, by considering simple processes for the two components of DOM.

In section 2, the model used in this study will be described. In section 3, case studies changing production rate and decay time of SDOM are made, and the horizontal and the vertical distribution of SDOC are discussed. The distribution of RDOC is also shown. The roles of DOM in the carbon and the nutrients cycle will be discussed based on the horizontal and the vertical flux of DOC. In section 4, the results are summarized.

2. Model

The model in this study is exactly the same as that in YT except the DOM processes (for details, see *Yamanaka* [1995] or YT). The horizontal resolution is 4°. There are 17 levels in the vertical, whose grid size increase with depth, from 50 m for the surface layer to 500 m for the deep layers. We adopt a realistic ocean bathymetry, but the Arctic Sea and Mediterranean Sea are not included. We use an off-line procedure; the tracer distributions are calculated using flow fields obtained by a separate ocean general circulation model (OGCM). The model in this study makes use of the flow fields and the distributions of temperature and salinity of the world ocean, which are obtained by the OGCM described by YT. We assumed the same values for horizontal and vertical diffusion coefficients as those in the general circulation model, whose values are $A_{HH} = 8 \times 10^2 \mathrm{m}^2/\mathrm{s}$ and $A_{HV} = 0.2 \times 10^{-4} \mathrm{m}^2/\mathrm{s}$, respectively. Export production due to POM is assumed to be a linear function of $L_f[\mathrm{PO_4}]$, where L_f is normalized light factor and $[\mathrm{PO_4}]$ is phosphate concentration in the surface layer. The vertical profile of POM downward flux is represented in the form of $(z/100\ \mathrm{m})^{-0.9}$.

We take into account two types of DOC, the semilabile DOC (SDOC) and the refractory DOC (RDOC). Prognostic variables in our model are as follows: the concentration of atmospheric CO_2, $^{13}CO_2$, $^{14}CO_2$, ocea-

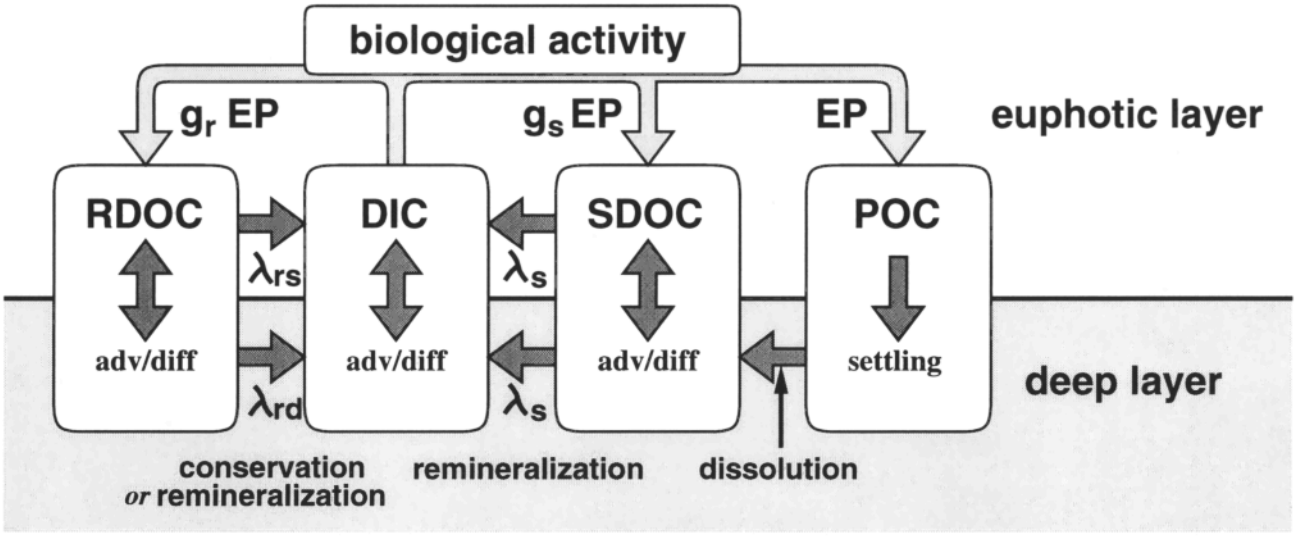

Figure 1. Production and consumption processes of semi-labile DOM (SDOM) and refractory DOM (RDOM) included in the biogeochemical general circulation model (BGCM).

nic total CO_2 (dissolved inorganic carbon, DIC), $DI^{13}C$, $DI^{14}C$, alkalinity, phosphate, dissolved oxygen, SDOC (SDOM), $SDO^{13}C$, $SDO^{14}C$, RDOC(RDOM), $RDO^{13}C$, and $RDO^{14}C$. Composition of DOM is assumed to have the same classical Redfield ratio as that of POM. The parameters and constants for the processes except the DOM processes are exactly the same as those in the control case of YT. The advection and diffusion of SDOC and RDOC are treated in the same manner as for the other chemical tracers.

The mechanisms of DOM production and consumption are not well known [*Kirchman et al.*, 1993]. In ecosystem modeling, various treatments of DOM production and consumption have been tested [e.g., *Fasham et al*, 1990; *Kawamiya et al.*, 1994]. Since their treatments are complicated and our purpose is to study the behavior of DOM in the global biogeochemical cycle, we treat the DOM production and consumption processes in the following simple way (Figure 1). The production rate of both SDOM and RDOM is assumed to be at a constant fraction g_s and g_r of POM, respectively. The g_s is assumed to have a value in the range of 0.5 to 4 (Table 1), as the observed production rate of SDOM is unknown. The decay time of SDOC, λ_s, is assumed to be in the range of 0.25 $\sim$ 20 years (Table 1). As will be discussed in section 3, the value of $\lambda_s = 0.5$ year is consistent with the fact that the observed DOC concentration shows seasonal variations [*Carlson et al.*, 1994]. POM is assumed to be dissolved into SDOM. It is reasonable that POM is remineralized into inorganic components through DOM. However, the ratio of flux passing through SDOM against that through labile DOM is not known, as the mechanisms of DOM production and consumption are not well known. We assume that all fraction of POM is dissolved into SDOM. In previous studies [e.g., *Bacastow and Maier-Reimer*, 1991], POM is assumed to be directly remineralized into inorganic components. This treatment can be considered as assuming that all POM is remineralized through labile DOM and that labile DOM is ignored, as its decay time is very short.

The important features of the DOC distribution in the deep water obtained from the observations are as follows: (1) the horizontal contrast of $(\Delta^{14}C)_{DOC}$ between the deep North Atlantic and the deep North Pacific is the same as that of DIC [*Bauer et al.*, 1992], (2) the DOC concentration is almost constant all the way from the deep North Atlantic to the deep Pacific [*Martin and Fitzwater*, 1992]. These features indicate that most of the DOC is conserved in the deep water; there are no net sources or sinks of DOC in the deep water on timescales shorter than the mixing time of the deep ocean. *Mopper et al.* [1991] suggested that the photochemical pathway is the rate-limiting step for the decomposition of RDOC in the sunlit layer above the depth of 5 m where light of ultraviolet B penetrates. Therefore RDOC is assumed to be conserved at depths below the euphotic layer, i.e., the decay time of RDOC in the deep water is assumed to be $\lambda_{rd} \rightarrow \infty$, and the consumption of RDOC is limited to the surface water. The global averaged turnover time of DOC is about 5000 years [*Bauer et al.*, 1992]. Combined with the ratio of the euphotic layer depth (50 m) against the global averaged depth of the seafloor, 3700 m, the decay time of RDOC in the euphotic layer is estimated to be about 70 years, i e , 5000 years $\times$ 50 m / 3700 m = 70 years

Table 1. Summary of Parameters for Numerical Experiments in This Study

Experiment	Semilabile		Refractory		
	g_s	λ_s	g_r	Surface λ_r	Deep λ_r
1	2.0	0.5	0.015	65	∞
2	2.0	0.5	0.012	80	∞
3	2.0	0.5	0.0195	50	∞
4	2.0	0.5	0.015	90	20000
5	2.0	0.5	0.015	150	10000
6	4.0	0.25		not considered	
7	3.0	0.25		not considered	
8	2.0	0.25		not considered	
9	1.0	0.25		not considered	
10	4.0	0.5		not considered	
11	3.0	0.5		not considered	
12	2.0	0.5		not considered	
13	1.0	0.5		not considered	
14	0.5	0.5		not considered	
15	3.0	1.0		not considered	
16	2.0	1.0		not considered	
17	1.0	1.0		not considered	
18	0.5	1.0		not considered	
19	2.0	2.0		not considered	
20	1.0	2.0		not considered	
21	0.5	2.0		not considered	
22	2.0	4.0		not considered	
23	1.0	4.0		not considered	
24	0.5	4.0		not considered	
25	2.0	10.0		not considered	
26	1.0	10.0		not considered	
27	0.5	10.0		not considered	
28	1.0	20.0		not considered	
29	not considered			not considered	

The g_s and g_r are the bioproduction efficiency ratio of semilabile DOM and refractory DOM against POM production, respectively, λ_s and λ_r are decay time of semilabile DOM and refractory DOM, respectively, g_s and g_r are nondimension parameters, and the units of λ_s and λ_r are years. Experiment 29 is same as the control case of *Yamanaka and Tajika* [1996].

We use the decay time of RDOC, λ_{rs}, to be 65 years in experiment 1 (Table 1). From the turnover time of about 5000 years and the stock size, about 700 Gt C, of DOC, the RDOC production rate is estimated to be 0.14 Gt C/yr. The production coefficient of RDOC, g_r, is assumed to be 0.015, as the POC production rate is about 8 Gt C/yr in experiment 1.

To investigate sensitivity of DOC distribution and $\Delta^{14}C$ to these parameters, we also calculate four cases in which the decay time constant in the deep layer, λ_{rd}, is 10,000 and 20,000 years and the decay time constant in the surface layer, λ_{rs}, is 150 and 50 years, respectively. We performed 29 experiments with various values of the model parameters. The parameters used for each case are listed in Table 1. We include both SDOC and RDOC in experiments 1–5, and only SDOC in experiments 6–28. The parameters in experiment 12 are taken to be the same as those in experiment 1 in order to examine the effect of RDOC. As will be discussed in section 3, RDOC does not affect the distribution of other chemical tracers. Experiment 29 is the same as the control case in YT, in which DOM is not included. We obtain the distribution of tracers for each case after carrying out the time integration for 4000 years for experiments 1–5 and 3000 years for experiments 6–29.

3. Results and Discussions

3.1. Horizontal Distribution of Semilabile DOC

Figure 2a shows the meridional SDOC distributions for five cases: experiments 8, 12, 16, 19, and 22, each with a different decay time constant, λ_s, and the observed SDOC concentrations of H. Ogawa and I. Koike (manuscript in preparaion, 1997) and *Peltzer and Hayward* [1996]. Since the observations do not determine the absolute value of SDOC and RDOC, we assume that the "observed SDOC" is considered to be the difference in DOC concentration between the surface and the deep water below a depth of 1000 m, as all of DOC in

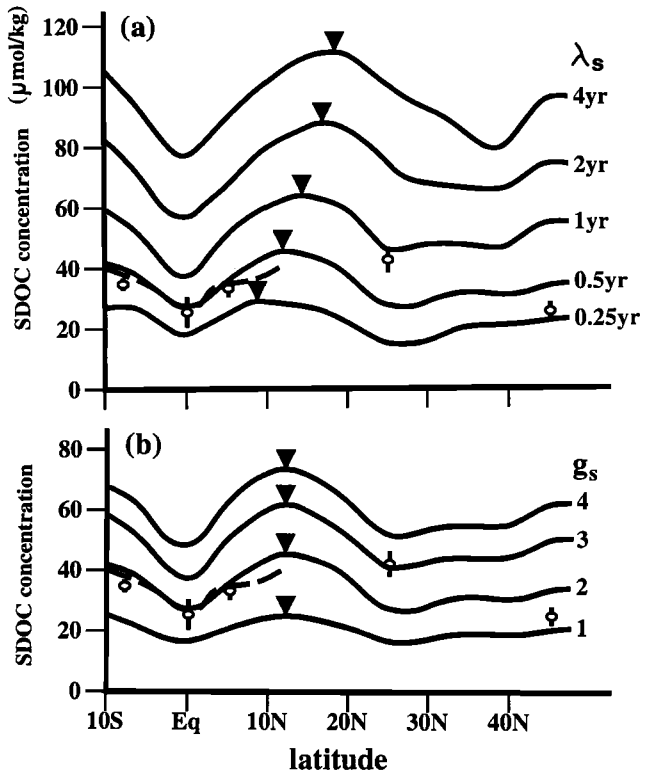

Figure 2. Meridional distribution of SDOC in the surface layer along the solid line in Figure 3 obtained in (a) experiments 8, 12, 16, 19, and 22, and (b) experiments 10–13. The solid lines from top to bottom in Figure 2a are for results in experiment 22 (λ_s = 4 years), experiment 19 (λ_s = 2 years), experiment 16 (λ_s = 1 year), experiment 12 (λ_s = 0.5 year), and experiment 8 (λ_s = 0.25 year). The solid lines from top to bottom in Figure 2b are for results in experiment 10 (g_s = 4.0), experiment 11 (g_s = 3.0), experiment 12 (g_s = 2.0), and experiment 13 (g_s = 1.0). Open circles are for the observations, 23 ± 3 μmol/kg (45°12'N,165°00'W on October 18, 1993), 42 ± 4 μmol/kg (24°32'N,169°00'W on October 25, 1993), 31 ± 3 μmol/kg (5°00'N,160°00'W on November 12, 1993), 25±5 μmol/kg (0°06'N,159°00'W on November 16, 1993), and 34±2 μmol/kg (8°00'N,160°00'W on November 15, 1993), respectively, by H. Ogawa and I. Koike (manuscript in preparation, 1997), and error bars are estimated from the deviation in the surface and the deep layer. Thick dashed line is from the observation from 12°S to 12°N along 140°W in February and March 1992, by *Peltzer and Hayward* [1996]. Triangles represent the maximum point of DOC concentration in each experiments. The observed SDOC concentration means the difference of DOC concentration between the surface and the deep layer below the depth of 1000 m.

the deep water is regarded as RDOC. This assumption will be verified in section 3.3. This procedure is used to avoid errors caused by different blank levels among the various laboratories. The SDOC concentrations obtained in all five cases have a minimum at the equator, as found in the observations. The model results also have a maximum at 9°N to 19°N, whose latitude depends on the decay time for SDOC. The maximum latitude increases with an increase of the decay time λ_s: 9°N for λ_s = 0.25 year (experiment 8) through 19°N for λ_s = 4 years (experiment 22). Although the average SDOC concentration along the section increases with an increase of the decay time, the ratio of the contrast against the average SDOC concentration along the section becomes smaller as the decay time increases,

Figure 2b shows the meridional SDOC distributions for the four cases, experiments 10–13, with different production coefficient, g_s, and the observed values [*Peltzer and Hayward*, 1996; H. Ogawa and I. Koike, manuscript in preparation, 1997]. The maximum of SDOC concentration obtained in the four cases is located at the same latitude. Although the average SDOC concentration along the section increases with an increase of production coefficient, the ratio of the contrast against the average SDOC concentration along the section is almost constant with different production ratio. This sensitivity of the production ratio is different from that of the decay time constant.

Thus, when the meridionally averaged SDOC concentration is held constant while changing of both parameters λ_s and g_s, the meridional contrast of the SDOC concentration becomes smaller as the decay time increases. The maximum tends to disappear with increasing the decay time. The SDOC concentration obtained in the case of $\lambda_s \geq 1.0$ year cannot reproduce the observed SDOC concentration, because the meridional contrast of the SDOC concentration is smaller than that observed, or because the meridional averaged SDOC concentration is larger than that observed. On the other hand, the SDOC concentration obtained in the case of λ_s = 0.25 year is not consistent with observations, as the maximum of SDOC concentration is located at 9°N, which is not found in the data of *Peltzer and Hayward* [1996]. Therefore the distribution obtained in the case of λ_s = 0.5 year and g_s = 2.0 compares best with the observation of H. Ogawa and I. Koike (manuscript in preparation, 1997) and *Peltzer and Hayward* [1996].

The observations by *Tanoue* [1992, 1993] in the Pacific show that the SDOC concentration has a double maximum at about 10°N and about 10°S with a minimum at the equator. Unfortunately, his HTC method is not the improved HTC method with appropriate corrections for the instrument blank after *Sharp* [1993]. The DOC concentrations of his observation have a larger value and larger error than those of more recent data [e.g., *Peltzer and Hayward*, 1996; H. Ogawa and I. Koike, manuscript in preparation, 1997]. However, the model results are qualitatively consistent with Tanoue's observations, although it is difficult to compare these quantitatively.

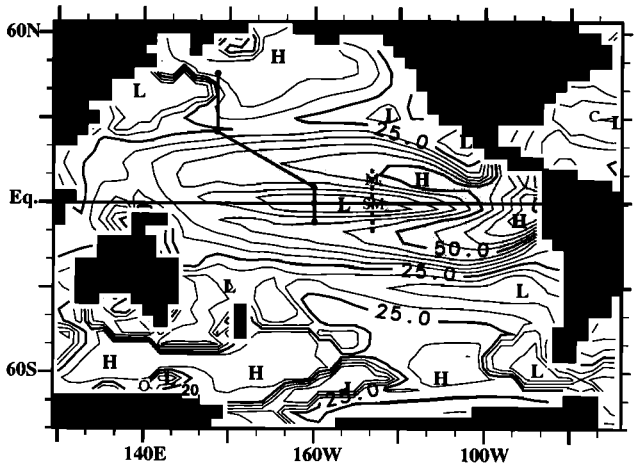

Figure 3. Horizontal distribution of SDOC in the surface Pacific obtained in experiment 1 and the observations. Solid line indicates location of meridional line in Figure 2. Dotted line indicates location of the observations by *Peltzer and Hayward* [1996]. Marks O, M_1, M_2, S, and C are for the observations 10 ± 5 μmol/kg (64°00'S, 140°00'E, on January 13, 1995) by H. Ogawa and I. Koike (manuscript in preparation, 1997), 60 ± 12 μmol/kg (9°00'N, 140°00'W, on June 25, 1990) and 20 ± 12 μmol/kg (0°04'N, 139°59'W, on July 1, 1990) by *Martin and Fitzwater* [1992], 28 ± 6 μmol/kg (9°00'N, 140°00'W, from March 25 trough April 9, 1992) by *Sharp et al.* [1995], and 14 ± 3 μmol/kg (31°50'N, 64°'10W and 32°10'N, 64°10'W from autumn 1991 through winter 1993) by *Carlson et al.* [1994], respectively. Contour intervals are 5 μmol/kg. Shaded area represents ≥ 40 μmol/kg.

Figure 3 shows the horizontal distribution of the SDOC concentration in the surface layer in experiment 1. The SDOC concentration in our model is consistent with the other observations [*Martin and Fitzwater*, 1992; *Carlson et al.*, 1994; *Sharp et al.*, 1995; *Peltzer and Hayward*, 1996; H. Ogawa and I. Koike, manuscript in preparation, 1997]. It is found that the double maximum of the SDOC concentration at 10°N and 10°S (Figure 3) extends in the east-west direction, i.e., a double DOC maximum zone (DDMZ) exists in the equatorial Pacific. Figure 4 illustrates the mechanism of the double DOC maximum zone. The surface water is diluted by SDOC poor water upwelled from the subsurface layer, although the SDOC production at the equator is highest. The surface water moves poleward with the Ekman transport. Then the maximum of the DOC concentration is located at the point where the production rate is balanced with the consumption rate The high SDOC concentration off the coast of Peru may be overestimated, as the flow field in this model does not reproduce the coastal upwelling. There are regions of low SDOC concentration at high latitudes, where SDOC is transported to the subsurface layer by convection, although SDOC production in these regions is higher than other regions in the same latitude.

From the comparison of the horizontal distribution of SDOC in our model with the observations, we obtain the optimal value for the decay time, $\lambda_s = 0.5$ year This timescale is much shorter than the horizontal mixing time in the surface water between the high-production and the low-production areas, because the model results with this timescale allow variations in the surface SDOC concentration. On the other hand, the surface concentration of RDOC is almost constant because the decay time is longer than the horizontal mixing time in the surface water. This will be discussed later.

3.2. Vertical Distribution of Semilabile DOC

Figure 5 shows the vertical SDOC concentration normalized by the surface SDOC concentration in the world ocean for the five cases: experiments 12, 16, 19, 22, and 25. It is found that SDOC penetrates into deeper layers for a longer decay time. The SDOC obtained in experiment 12 with $\lambda_s = 0.5$ year, is limited above the depth of 400 m, whose vertical profiles compare well

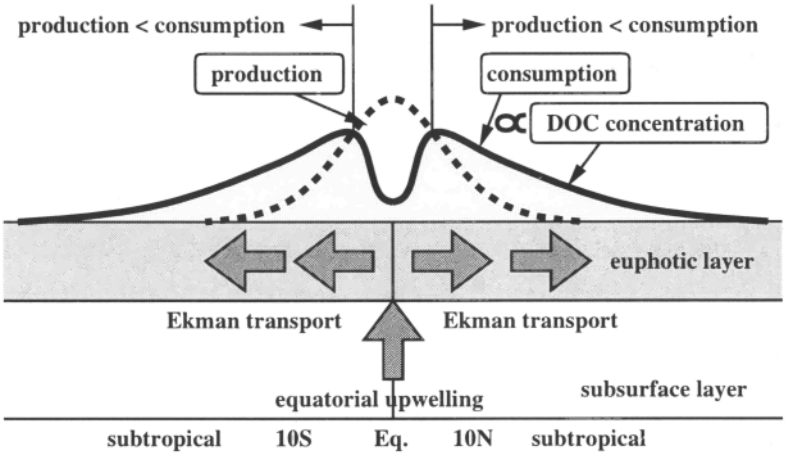

Figure 4. Illustration of mechanism of DOC double maximum zone

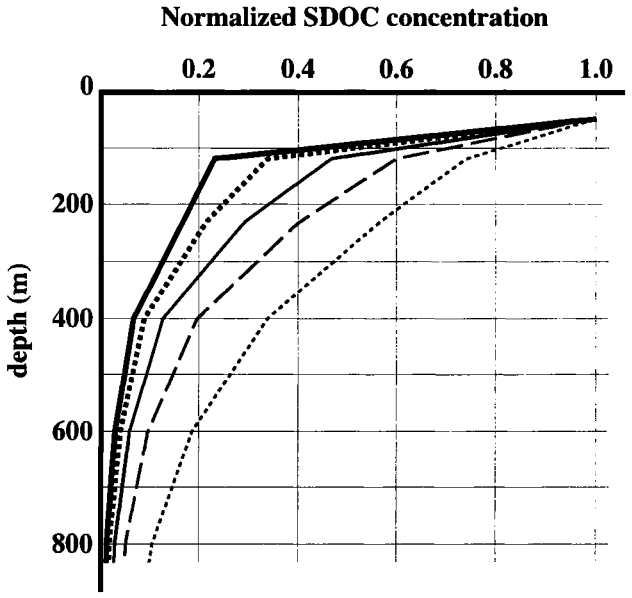

Figure 5. Horizontally averaged vertical distribution of SDOC concentration normalized by the surface SDOC concentration in the world ocean. Thick solid line, thick dotted line, thin solid line, thin dashed line, and thin dotted line are for experiments 12, 16, 19, 22, and 25, respectively.

with the observations [e.g., *Tanoue*, 1993]. In order to compare objectively the calculated vertical profiles of SDOC with the observations, we consider the surface concentration and the penetration depth of SDOC for each case. The penetration depth is defined as the vertically integrated concentration divided by the surface concentration. Figure 6a shows the horizontally averaged surface SDOC concentration in the world ocean for each case in the SDOC production coefficient – decay time plane. The SDOC concentration increases with an increase of both the SDOC production ratio and the decay time. The observed values are about 15 μmol/kg (H. Ogawa and I. Koike, manuscript in preparation, 1997) through 40 μmol/kg [*Tanoue*, 1993]. When both the SDOC production ratio and the decay time are within the range of the shaded area in Figure 6a, the observed concentration of the surface SDOC is well reproduced. Figure 6b shows the globally averaged penetration depth for each case. The penetration depth increases with smaller SDOC production ratio and with longer decay time. The former is due to maintenance of SDOC by the dissolution of POC at depths below the euphotic layer. In experiment 12, half of SDOC at those depths is produced from the dissolution of POC. The observed penetration depth is about 100~150 m. When the production ratio and the decay time are within the shaded area in Figure 6b, the observed penetration depth is well reproduced. From the vertical SDOC distribution, the optimal values for the SDOC production ratio g_s and the decay time λ_s are within the solid oval area, i.e., about $\lambda_s \simeq 0.5$ and about $g_s \simeq 2.0$, respectively. When POM is assumed to be directly remineralized into the inorganic components, the optimal values are shifted to about $\lambda_s \simeq 1.0$ and about $g_s \simeq 1.0$.

From the above discussion of the horizontal and the vertical SDOC distribution, we can constrain the optimal values for the SDOC production ratio g_s and the decay time λ_s to be $\lambda_s \simeq 0.5$ and $g_s \simeq 2.0$, respectively. Further improvement of the model and intensive observations of DOM are required for determination of more precise values both of the SDOM decay time and SDOM production rate. The effect of vertical numerical diffusion in the model leads to an overestimate of the SDOM penetration depth in the model. The effect of the DOM with an intermediate decay time between SDOM and RDOM would cause the observed SDOM penetration depth to be underestimated, if it exists in significant amounts. In order to obtain a more precise observed penetration depth, intensive observations in various regions at a depth of 100 to 400 m are required.

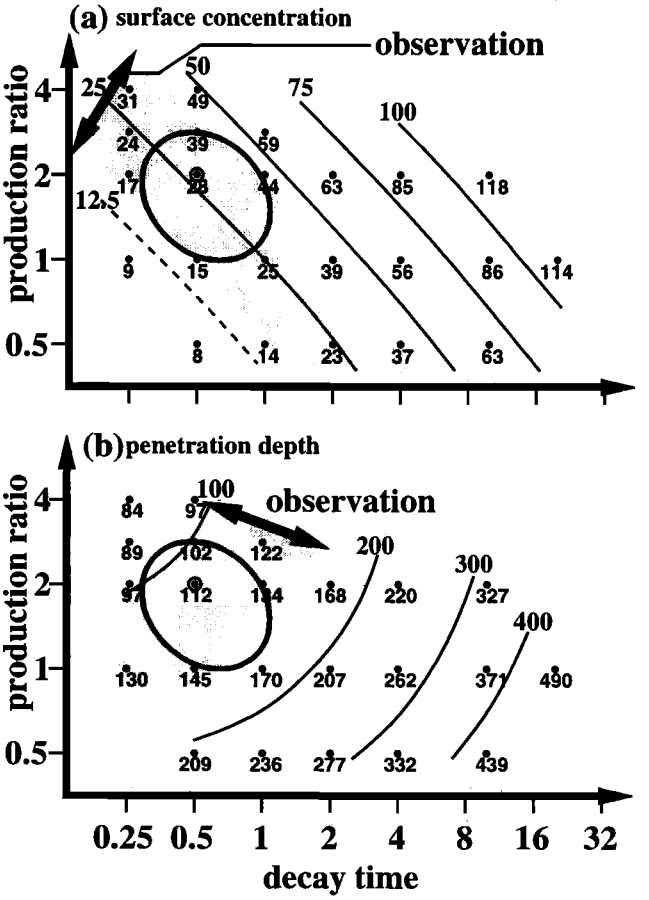

Figure 6. Horizontally averaged (a) surface concentration and (b) penetration depth of SDOC in the world ocean. Shaded area represents the range of observation. Solid oval represents the best fit area to the observation.

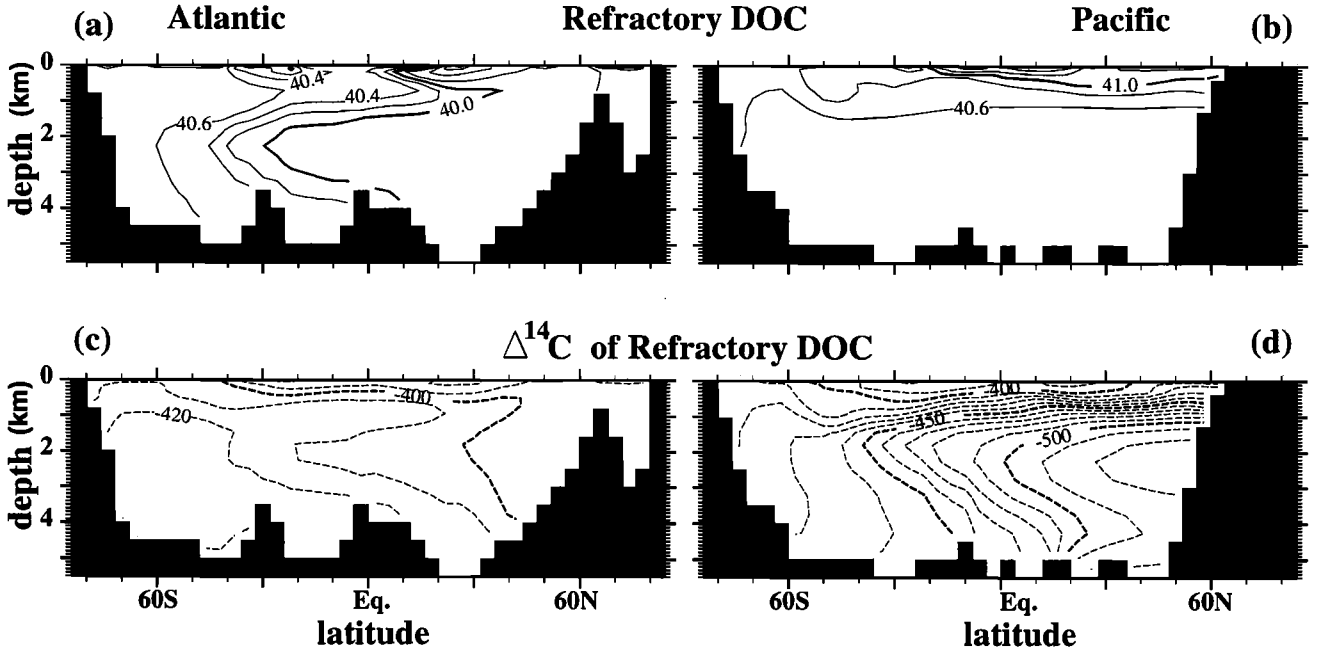

Figure 7. (a) and (b) Refractory DOC concentration (contour intervals of 0.2 μmol/kg) and (c) and (d) the $\Delta^{14}C$ values of refractory DOC (contour intervals of 10 ‰) along the GEOSECS sections in (left) the western Atlantic and (right) the western Pacific in experiment 1.

3.3. Distribution of Refractory DOC

Figure 7 shows the RDOC concentration and its $\Delta^{14}C$ values along the GEOSECS sections in the western Atlantic and the western Pacific obtained in experiment 1. The RDOC concentration is almost constant at about 40 μmol/kg. The production rate of RDOC is about 0.15 Gt C/yr. The turnover time, RDOC stock size/production rate, in the surface layer is estimated to be about 70 years, which is equal to the RDOC decay time in the surface layer. The RDOC concentration is almost constant not only in the deep water but also in the surface water. Although the RDOC production in the equator region and at high latitudes is about 1 order higher than that in the subtropical gyre, the timescale of about 70 years is long with respect to the mixing time between the high-production and the low-production area in the surface water. Since the RDOC concentration is almost constant, it is reasonable to assume the difference in DOC concentration between the surface and the deep water is due to the SDOC concentration. The distribution of $(\Delta^{14}C)_{RDOC}$ in the deep water is similar to DIC except that its value is 300‰ lower. This difference is due to the 300‰ difference of $\Delta^{14}C$ between RDOC and DIC in the surface water, which is due to the difference rate between RDOC production in the surface layer and CO_2 gas exchange through the ocean surface. The RDOC turnover time in the surface layer of about 70 years is much longer than the DIC turnover time of about 6 years determined from the ratio of the DIC concentration to the CO_2 gas exchange rate. That is, the recovery from old $(\Delta^{14}C)_{SDOC}$ upwelled from the deep layer into the fresh $(\Delta^{14}C)_{SDOC}$ of -50‰ is much slower than that from old $(\Delta^{14}C)_{DIC}$ into 0‰ .

Figure 8 shows vertical profiles of the $(\Delta^{14}C)_{DOC}$ and $(\Delta^{14}C)_{DIC}$ in the Sargasso Sea and the North Pacific for the model and the observations of *Bauer et al.* [1992]. The model results of $(\Delta^{14}C)_{DIC}$ in the deep North Atlantic and the deep North Pacific are about -70‰ and about -240‰, respectively, which are similar to the observations. The calculated values for $(\Delta^{14}C)_{DOC}$ in the North Atlantic and the North Pacific are about -400‰ about -520‰, respectively, which are also similar to the observations. The model $(\Delta^{14}C)_{DOC}$ in the surface water is about -270‰, which is a combination of $(\Delta^{14}C)_{RDOC}= -390$‰ with $(\Delta^{14}C)_{SDOC}= -50$‰. The calculated value in the surface water is lower than the observed by about 70‰, because of lack of the bomb ^{14}C effect. With inclusion of the bomb ^{14}C effect, the calculated $(\Delta^{14}C)_{DOC}$ is about -200‰, which is close to the observations (not shown). The horizontal contrast of $(\Delta^{14}C)_{DOC}$ between the North Atlantic and the North Pacific, 110‰, is smaller than that of $(\Delta^{14}C)_{DIC}$, 170‰. However, in the $\Delta^{14}C$ age scale, the horizontal contrast of $(\Delta^{14}C)_{DOC}$, 1800 years, is almost the same as that of $(\Delta^{14}C)_{DIC}$, 1700 years.

From the above discussion, RDOC in the deep water is roughly considered to be conserved. We discuss the sensitivity of the RDOC concentration and

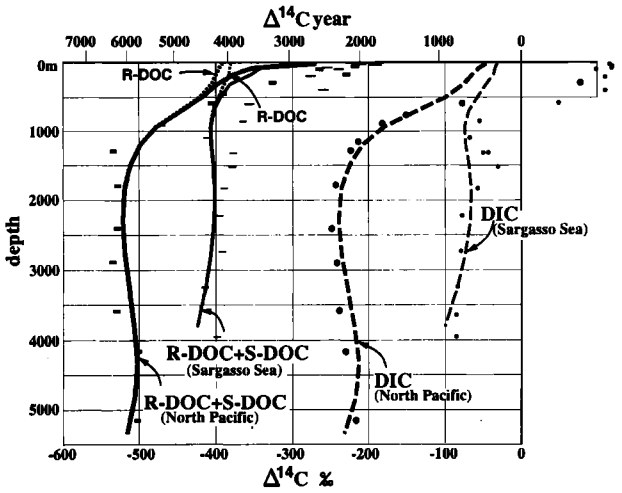

Figure 8. Vertical profiles of the $\Delta^{14}C$ values of DOC and DIC. Thick and thin dashed lines are for model results of DIC in the North Pacific (32°N,160°W) and the Sargasso Sea (32°N,64°W), respectively. Thick and thin solid lines are for model results of total DOC which is sum of RDOC and SDOC in the North Pacific and the Sargasso Sea, respectively. Thick and thin dotted lines are for model results of RDOC in the North Pacific and the Sargasso Sea, respectively. Solid circle and thick bar are for observations of DIC and DOC in the North Pacific, and open circle and thin bar are for these in the Sargasso Sea [*Druffel et al.*, 1992].

$(\Delta^{14}C)_{RDOC}$ to two parameters, λ_{rs} and λ_{rd}, in the rest of this subsection.

Figure 9 shows the vertical $(\Delta^{14}C)_{RDOC}$ distribution in the North Pacific and the North Atlantic obtained in the three cases: experiments 1–3 with different two parameters, g_r and λ_{rs}, under the condition of $g_r\lambda_{rs}$ = const. Since the ratio of the production rate against the consumption rate is almost constant, total RDOC concentration in the world ocean is kept almost constant. The RDOC concentration obtained in the three cases is almost the same from the North Atlantic to the North Pacific (not shown). The absolute $(\Delta^{14}C)_{RDOC}$ value increases with increasing the production and the consumption rate, as the turnover time of RDOC is quicker. However, the relative difference of RDOC ^{14}C year between the North Pacific and the North Atlantic is almost the same among the three cases. From these case studies, it is found that the relative difference of RDOC concentration and $(\Delta^{14}C)_{RDOC}$ between the deep North Pacific and the deep North Atlantic cannot be controlled by the parameters in the surface layer, g_r and λ_{rs}, under the assumption that RDOC is conserved in the deep layer.

Figure 10 shows the vertical distributions of RDOC in the North Pacific and the North Atlantic obtained in the three cases: experiments 1, 4, and 5 with different two parameters, λ_{rs} and λ_{rd}, under the condition of the fixed production rate constant, g_r = const. The two parameters λ_{rs} and λ_{rd} are adjusted so as to fit the globally averaged RDOC concentration of about 40 μmol C/kg. The RDOC concentration in the deep North Pacific decreases with a decrease of the decay time in the deep layer. On the other hand, the RDOC concentrations in the surface layer and the deep North Atlantic increase, because the decay time in the surface layer increases. The difference of the RDOC concentration between the deep North Pacific and the deep North Atlantic obtained in experiment 5 is 4 to 6 μmol C/kg. The error due to the blank control of the recent observations by the HTC method is within 10 μmol C/kg [*Sharp et al.*, 1995]. Therefore the RDOC decay time in the deep layer is estimated to be longer than 10,000 years under the error range of the recent observations. In experiments 4 and 5, the RDOC concentration in the North Pacific increases from a depth of 2000 m toward the surface layer. This is consistent with recent obser-

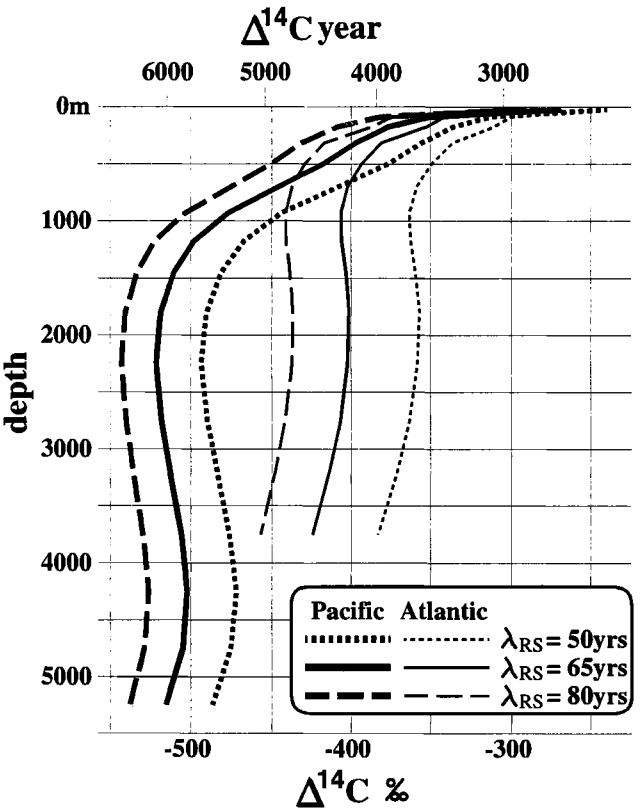

Figure 9. Vertical profiles of the RDOC $\Delta^{14}C$ values in the North Pacific (32°N,160°W) and the North Atlantic (32°N,64°W). Thick solid line, thick dashed line, and thick dotted line are for $(\Delta^{14}C)_{RDOC}$ in the North Pacific obtained in experiment 1, experiment 2, and experiment 3, respectively. Thin solid line, thin dashed line, and thin dotted line are for $(\Delta^{14}C)_{RDOC}$ in the North Atlantic obtained in experiment 1, experiment 2, and experiment 3, respectively.

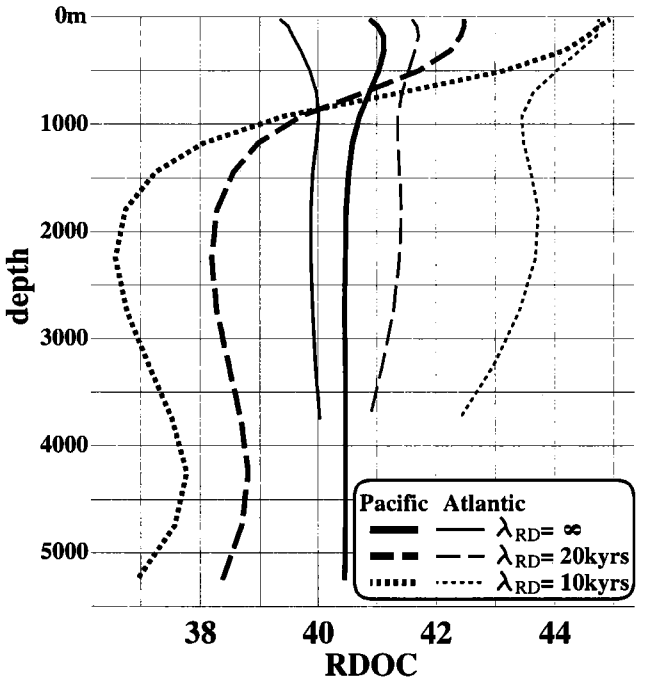

Figure 10. Vertical profiles of the RDOC concentration in the North Pacific (32°N,160°W) and the North Atlantic (32°N,64°W). Thick solid line, thick dashed line, and thick dotted line are for the RDOC concentration in the North Pacific obtained in experiments 1, 4, and 5, respectively. Thin solid line, thin dashed line, and thin dotted line are for the RDOC concentration in the North Atlantic obtained in experiments 1, 4, and 5, respectively.

vations in the Pacific [*Peltzer and Hayward*, 1996; H. Ogawa and I. Koike, manuscript in preparation, 1997]. That is, there is a possibility that the RDOC remineralization with a long decay time constant in the deep layer can explain the observed vertical DOC distribution at depths between 400 m and 1500 m in the Pacific.

Since the production rate and the globally averaged RDOC concentration are almost the same among the three cases, the $(\Delta^{14}C)_{RDOC}$ distribution is almost the same. Strictly speaking, the $(\Delta^{14}C)_{RDOC}$ in the deep North Pacific obtained in experiment 5 is about 10‰ younger than that in experiment 1, and the difference of $(\Delta^{14}C)_{RDOC}$ between the deep North Pacific and the deep North Atlantic obtained in experiment 5 is about 10‰ smaller (not shown). This is because the exchange rate of RDOC due to the advection and diffusion between the surface and the deep water in experiment 5 is larger than that in experiment 1, as the RDOC concentration in the deep North Pacific in experiment 5 is smaller. Therefore the $(\Delta^{14}C)_{RDOC}$ in the deep North Pacific with the RDOC remineralization in the deep water is younger than that without the RDOC remineralization.

Last, we discuss the assumption that POM is significantly dissolved into RDOM in the deep layer. If this assumption is combined with the remineralization of RDOC into DIC as discussed above, the relative difference of RDOC concentration between the deep North Pacific and the deep North Atlantic can be controlled by tuning the dissolution rate of POM and the remineralization rate of RDOC. However, the $(\Delta^{14}C)_{RDOC}$ in the deep Pacific with this combination is necessarily younger than that in the case where the conservation of RDOC is assumed. As discussed above, the $(\Delta^{14}C)_{RDOC}$ difference between the North Pacific and the North Atlantic obtained in experiment 1, the case where the conservation of RDOC is assumed, is almost the same as the observed $(\Delta^{14}C)_{RDOC}$ difference. Therefore the assumption that POM is dissolved into RDOM in the deep layer seems to be inconsistent with the observations of *Bauer et al.* [1992].

From the above discussion of the RDOC concentration and $(\Delta^{14}C)_{RDOC}$, we can estimate that the RDOM decay time in the deep layer is longer than 10,000 years under the error range of the recent observations. The RDOM in the deep water is considered to be conserved as a first approximation. However, the RDOC remineralization with a long decay time constant in the deep layer may explain the observed vertical DOC distribution at depths between 400 m and 1500 m in the Pacific.

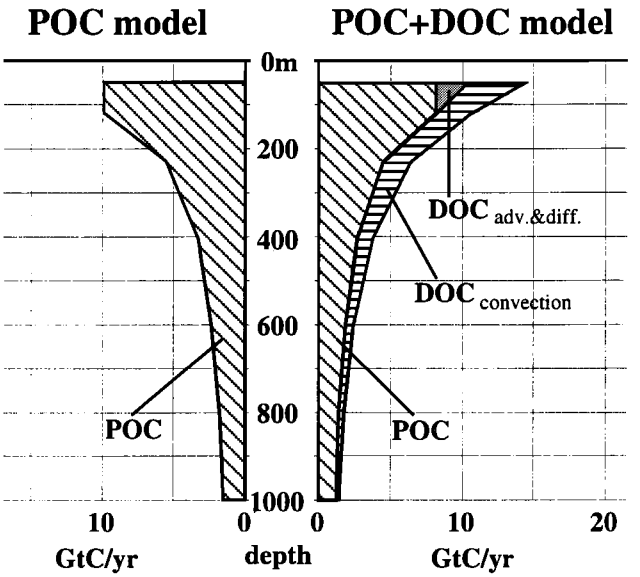

Figure 11. Horizontal averaged vertical carbon fluxes due to POC, advection and diffusion of SDOC ($DOC_{adv\&diff}$), and convective adjustment of SDOC (DOC_{conv}) in the world ocean in (right) experiment 1 andd in (left) experiment 29. Flux of RDOC is almost zero, as it is at the steady state and RDOC does not decay below the euphotic layer.

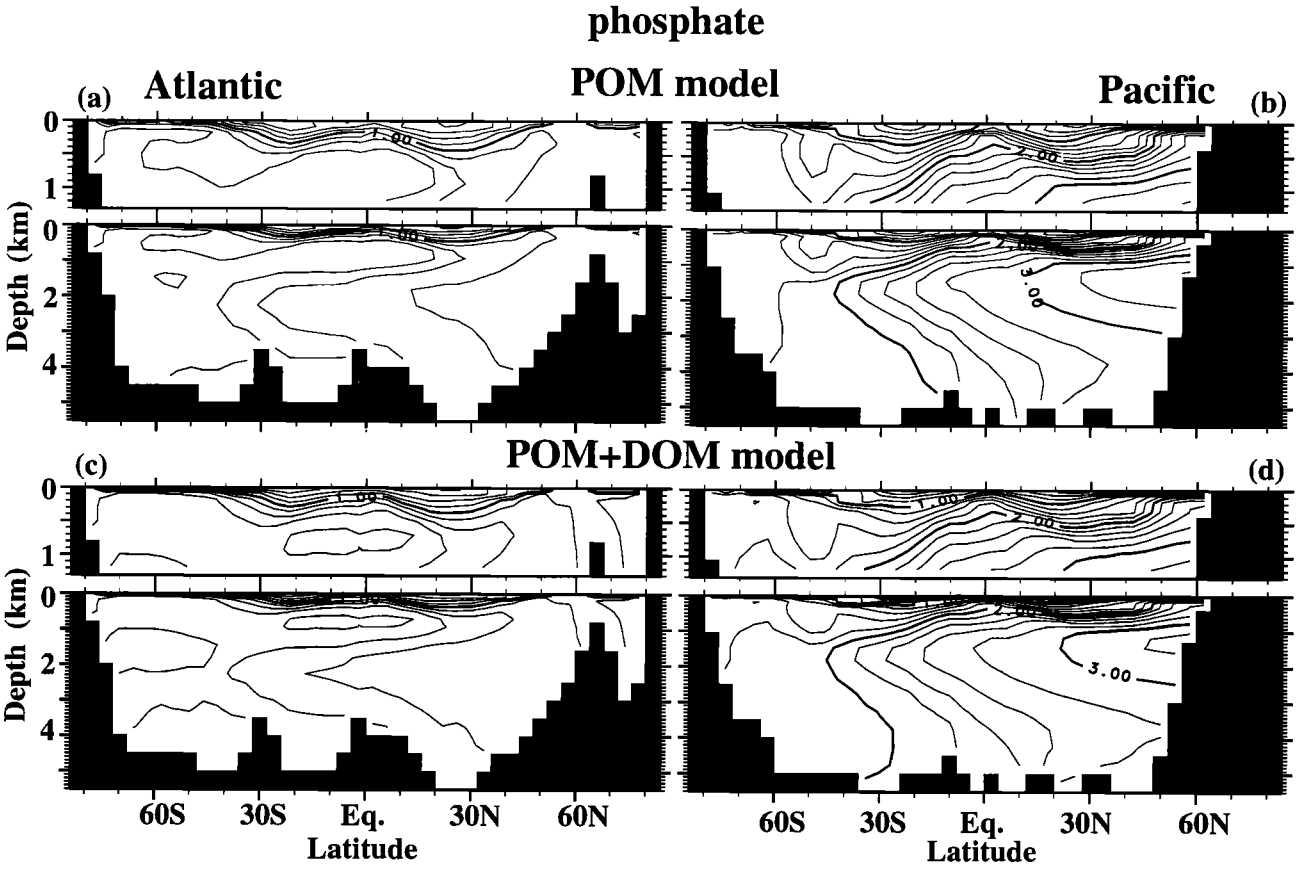

Figure 12. Phosphate distribution along the GEOSECS sections in (left) the western Atlantic and (right) the western Pacific in BGCM with (a) and (b) only POM, and (c) and (d) both POM and DOM. Contour intervals is 0.1μmol/kg.

3.4. Role of DOC in carbon cycle

Figure 11 shows the global vertical flux of carbon. The downward carbon transport is categorized into the three components, POC flux, DOC flux due to advection/diffusion, and DOC flux due to convection. The flux of RDOC is almost zero, as it is almost at steady state and RDOC is conserved below the euphotic layer. Even if RDOC decays in the deep water, the downward RDOC transport is estimated to be much smaller than POC and SDOC, which is about 0.06 Gt C/yr as obtained in experiment 5. The export production, which is defined as the vertical transport of POC at a depth of 100 m, is about 8.1 Gt C/yr in experiment 1. It is smaller than the value of about 9.9 Gt C/yr in experiment 29. These results are well within the estimated range of 4 to 20 Gt C/yr [*Eppley*, 1989; *Packard et al.*, 1988]. The export production due to DOC is estimated to be 3.3 Gt C/yr. It is in the range of 2.0 to 5.5 Gt C/yr with production ratio g_s = 1.0 to 3.0. High proportion of the DOC export production is due to convection, which is consistent with the recent observation [*Carlson et al.*, 1994]. The SDOM decay time of 0.5 year is shorter than the timescale of exchange due to advection/diffusion between the surface and the subsurface water, but it is longer than that of exchange due to convection.

The values below a depth of 400 m may be overestimated, as the convection in our model is represented by convective adjustment, which instantaneously mixes unstably stratified layers. Convection reaching below the depth of 400 m is limited to the Greenland Sea and the Weddel Sea, and the effect of the vertical DOM transport due to convection should be limited to these areas. In other regions, the vertical DOM transport is considered to be limited to depths above 400 m. Therefore we can conclude that the important role of DOM in the vertical carbon transport is restricted above a depth of 400 m, and the downward transport below this depth is due almost entirely to POC settling.

Figure 12 shows the distribution of the phosphate concentration along the GEOSECS sections in the western Atlantic and the western Pacific obtained in experiments 1 and 29, which reproduce the observations well (see Figure 9 of YT). The distribution of phosphate in experiment 1 is similar to that in experiment 29, al-

though the horizontal contrast between the deep North Pacific and the deep North Atlantic in experiment 1 is slightly smaller than that in experiment 29. The phosphate concentration in the region where the concentration is higher than the total averaged concentration, 2.1 μmol P/kg, in experiment 1 is lower than that in experiment 29. On the other hand, the phosphate concentration in the region where the concentration is lower than the total averaged concentration in experiment 1 is higher. This is because the export production due to POC in experiment 1 is smaller than experiment 9 (see Figure 11), and the downward transport of carbon below a depth of 400 m is due almost entirely to POM, which makes the horizontal contrast between the deep North Pacific and the deep North Atlantic; that is, the phosphate transport due to DOM downward flux does not play a role in the phosphate cycle below the depth of 400 m.

However, above a depth of 400 m, DOM plays an important role in the biogeochemical cycles. DOM is carried by the Ekman transport from the equatorial to the subtropical region, as discussed in the mechanism of DDMZ (Figure 4). This transport results in reduction of the "nutrient trapping" of *Najjar et al.* [1992]. Since this organic phosphate transport in the surface layer is comparable with the inorganic phosphate transport, the maximum value of the surface phosphate concentration in the equatorial region in experiment 1 (with DOM processes) is smaller than that in experiment 29 (without DOM processes). The phosphate concentration in the surface eastern equatorial Pacific is reduced from 2.4 μmol P/kg in experiment 29 to 1.5 μmol P/kg in experiment 1 (Figure 13). The phosphate concentration in the eastern equatorial Pacific at a depth of 700 m is also reduced from 4.8 μmol P/kg in experiment 29 to 4.0 μmol P/kg in experiment 1. The DOM transport due to the Ekman transport is thus important for reducing the nutrient trapping effect in the high-production areas, and for supplying nutrient to the low-production areas. The phosphate concentration in the surface high latitude in both cases is underestimated (Figure 13). This is probably due to the lack of the iron limitation effect, which is not included in our model, or the lack of the convection in winter, which transports the phosphate rich subsurface water into the surface layer, as the model in this study uses annual mean data as the surface boundary condition.

The distribution of other chemical tracers in experiment 12 is almost the same as that in experiment 1 (not shown in this paper), which suggests that RDOC may not play an active role in the carbon cycle. The RDOC concentration is estimated to be about 40 μmol C/kg, and its amount cannot be ignored as a carbon stock size in the ocean. However, the RDOM production and consumption rates are much smaller than the other fluxes

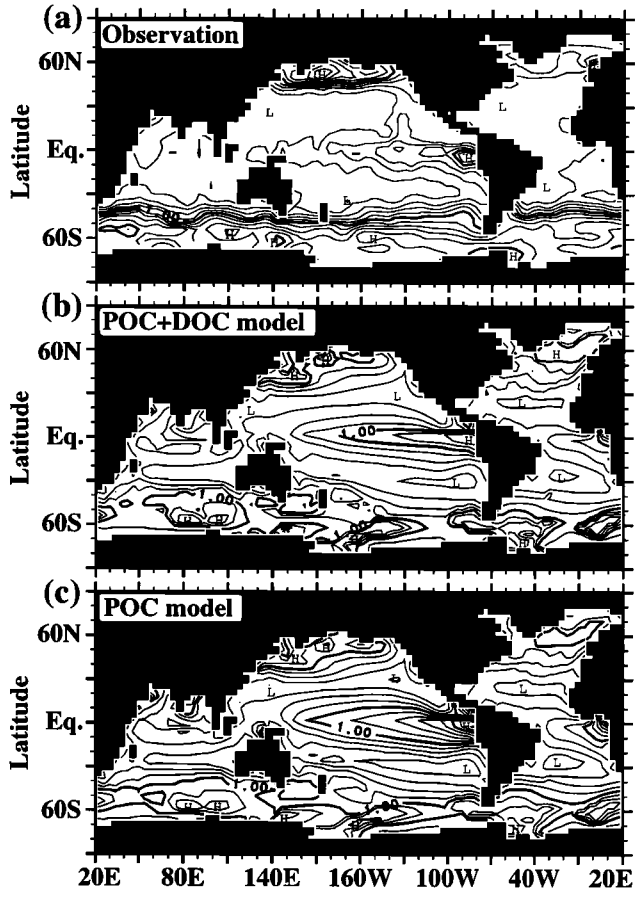

Figure 13. Phosphate distribution in the surface layer from (a) observation, (b) experiment 1, and (c) experiment 29. Contour interval is 0.2 μmol/kg.

such as the export production due to POM and SDOM. RDOM does not affect the distributions of other chemical tracers.

4. Conclusion

We have developed a biogeochemical general circulation model which includes DOM production and consumption processes. The semilabile and the refractory DOC are taken into account. The following observed features of DOC are well reproduced: (1) the DOC concentration decreases with depth and is almost constant below a depth of 400 m [e.g., *Tanoue*, 1992, 1993; *Martin and Fitzwater*, 1992; *Peltzer and Hayward*, 1996; H. Ogawa and I. Koike, manuscript in preparation, 1997], (2) horizontal variation of the DOC concentration in the surface water is in the range from 0 to 40 μmol C/kg [*Peltzer and Hayward*, 1996; H. Ogawa and I. Koike, manuscript in preparation, 1997] or 0 to 60 μmolC/kg [*Tanoue*, 1992, 1993], (3) the timescale of the DOC consumption permits seasonal variations and DOC is mainly transported by convection [*Carlson et al.*, 1994],

(4) the DOC concentration in the deep water is almost constant, 40 μmol C/kg, from the North Atlantic to the North Pacific [*Martin and Fitzwater*, 1992; H. Ogawa and I. Koike, manuscript in preparation, 1997], and (5) the age of DOC in the deep water is very old; that is, $\Delta^{14}C$ values in the North Atlantic and the North Pacific are about $-400‰$ and $-500‰$, respectively [*Bauer et al.*, 1992].

The optimal values for the decay time and the production coefficient of DOM (against POM) to explain the observation are estimated to be about 0.5 year and about two, respectively. In this study, POM is assumed to be remineralized into inorganic components through SDOM. When POM is assumed to be remineralized through labile DOM, the optimal values for the decay time and the production coefficient of DOM are slightly modified to be about 1 year and about one, respectively. That is, our conclusion that the decay time is much shorter than that in the previous studies [e.g., *Bacastow and Maier-Reimer*, 1991] is not changed by this assumption. The semilabile DOM exists only above a depth of 400 m, where its vertical and horizontal transport plays an important role in the oceanic carbon cycle. Intensive observations of DOM at depths between 100 m and 400 m in various regions are required for further understanding the role of DOM in the marine biogeochemical cycle in order to obtain a more precise observed penetration depth. The distribution of DOC in the surface layer shows that the double DOC maximum zone (DDMZ) extends in the east-west direction in the equatorial Pacific. The semilabile DOM production is estimated to be about 16 Gt/yr. In order to confirm this estimation of DOM production, we should further improve the DOM processes in our model because the DOM production processes in this study are simplified.

The production rate of the refractory DOC in the surface layer is estimated to be 0.14 Gt C/yr. The decay time of the refractory DOM in the surface layer is estimated to be about 65 years, and the refractory DOM is conserved below that layer as the first approximation. However, there is a possibility that the RDOC remineralization with a long decay time constant in the deep layer can explain the recent observed vertical DOC concentration at depths between 400 m and 1500 m in the Pacific [*Peltzer and Hayward*, 1996; H. Ogawa and I. Koike, manuscript in preparation, 1997]. The role of the refractory DOC in the carbon cycle is not important because the production and the decay rate of the refractory DOM are much smaller than those of the semilabile DOM and POM, and the refractory DOM does not decay below the surface layer.

The global export production due to POC and DOC at a depth of 100 m is about 8 Gt C/yr and about 3 Gt C/yr, respectively. However, the vertical carbon transport below 400 m is due almost entirely to POC.

Acknowledgments. We would like to thank Nobuo Suginohara for his helpful discussion and encouragements. We would also like to thank Hiroshi Ogawa for his comments and for giving us his data. The discussion of Jorge L. Sarmiento on the comparison of our model results with the previous model helped us to improve this paper. The suggestion of David Archer on the interpretation of our model results was very useful for improving this paper. The comments of anonymous reviewers were very helpful. Thanks are extend to E. Tanoue, T. Nagata, Y. Suzuki, E. Peltzer, I. Koike, and M. Kawamiya for their helpful discussions and comments. H. Mizukami helped us to make figures. Numerical calculations were performed by HITAC M-3800 at the Computer Center of the University of Tokyo. Figures were produced by GFD-Dennou Libraries on SUN Microsystems IPX.

References

Anderson, L.A., and J. L. Sarmiento, Global ocean phosphate and oxygen simulations, *Global Biogeochem. Cycles*, *9*, 621-636, 1995.

Bacastow, R., and E. Maier-Reimer, Ocean-circulation model of the carbon cycle, *Clim. Dyn.*, *4*, 95-125, 1990.

Bacastow, R., and E. Maier-Reimer, Dissolved organic carbon in modeling oceanic new production, *Global Biogeochem. Cycles*, *5*, 71-85, 1991.

Bauer, J.E., P.M. Williams, and E.R.M. Druffel, ^{14}C activity of dissolved organic carbon fractions in the north-central Pacific and Sargasso Sea, *Nature*, *357*, 667-670, 1992.

Carlson, C.A., H.W. Ducklow, and A.F. Michaels, Annual flux of dissolved organic carbon from the euphotic zone in the northwestern Sargasso Sea, *Nature*, *371*, 405-408, 1994.

Druffel, E.R.M., P.M. Williams, J.E. Bauer, and J.R. Ertel, Cycling of dissolved and particulate organic matter in the open ocean, *J. Geophys. Res.*, *97*, 15639-15659, 1992.

Eppley, R.W., History, methods, problems, in *Productivity of Ocean: Present and Past*, edited by V.S. Smetacek, G. Wefer, and W.H. Berger, pp. 85-97, John Wiley, New York, 1989.

Fasham, M.J.R., H.W. Ducklow, and S.M. NcKelvie, A nitrogen-based model of plankton dynamics in the oceanic mixed layer, *J. Mar. Res.*, *48*, 591-639, 1990.

Kawamiya, M., M. Kishi, Y. Yamanaka, and N. Suginohara, An ecological-physical coupled model applied to Station Papa, *J. Oceanogr.*, *51*, 635-664, 1994.

Kirchman, D.L., C. Lancelot, M. Fasham, L. Legendre, G. Radach, and M. Scott, Dissolved organic matter in biogeochemical models of the ocean, in *Towards a Model of Ocean Biogeochemical Processes*, edited by G.T. Evans and M.J.R. Fasham, *NATO ASI Ser. I, 10*, 209-225, 1993.

Maier-Reimer, E., Geochemical cycles in an ocean general circulation model. preindustrial tracer distributions, *Global Biogeochem. Cycles*, *7*, 645-677, 1993.

Martin, J.H., and S.E. Fitzwater, Dissolved organic carbon in the Atlantic, Southern and Pacific Oceans, *Nature*, *356*, 699-700, 1992.

Matear, R.J., and G. Holloway, Modeling the inorganic phosphorus cycle of the North Pacific using an adjoint data assimilation model to assess the role of dissolved organic phosphorus, *Global Biogeochem. Cycles*, *9*, 101-119, 1995.

Mopper, K., X. Zhou, R.J. Kieber, D.J. Kieber, R.J. Sikorski, and R.D. Jones, Photochemical degradation of dis-

solved organic carbon and its impact on the oceanic carbon cycle, *Nature*, *353*, 60-62, 1991.

Najjar, R.G., J.L. Sarmiento, and J.R. Toggweiler, Downward transport and fate of organic matter in the ocean: Simulations with a general circulation model, *Global Biogeochem. Cycles*, *6*, 45-76, 1992.

Packard, T.T., M. Denis, and P.L. Garfield, Deep-ocean metabolic CO_2 production: Calculations from ETS activity, *Deep Sea Res.*, *35*, 371-382, 1988.

Peltzer, E.T., and N.A. Hayward, Spatial and temporal variability of total organic carbon along 140°W in the equatorial Pacific Ocean in 1992, *Deep Sea Res. II*, *43*, 1155–1180, 1996.

Sharp, J.H., The dissolved organic carbon controversy: An update, *Oceanography*, *6*, 45-50, 1993.

Sharp, J.H., R. Benner, L. Bennett, C. A. Carlson, S. E. Fitzwater, E. T. Peltzer, and L. M. Tupas, Analyses of dissolved organic carbon in seawater: The JGOFS EqPac methods comparison, *Mar. Chem.*, *48*, 91-108, 1995.

Siegenthaler, U., and J.L. Sarmiento, Atmospheric carbon dioxide and the ocean, *Nature*, *365*, 119-125, 1993.

Sugimura, Y., and Y. Suzuki, A high-temperature catallytic oxidation methods for determination of nonvolatile dissolved organic carbon in seawater by direct injection of a liquid sample, *Mar. Chem.*, *24*, 105-131, 1988.

Suzuki, Y., On the measurement of DOC and DON in seawater, *Mar. Chem.*, *41*, 287-288, 1993.

Suzuki, Y., Y. Sugimura, and T. Itoh, A catalytic oxidation method for the determination of total nitrogen dissolved in seater, *Mar. Chem.*, *16*, 83-97, 1985.

Tanoue, E., Vertical distribution of dissolved organic carbon in the North Pacific as determined by the high-temperature catalytic oxidation method, *Earth Planet. Sci. Lett.*, *111*, 201-216, 1992.

Tanoue, E., Distributional characteristics of DOC in the central equatorial Pacific, *J. Oceanogr.*, *49*, 625-636, 1993.

Toggweiler, J.R., and J. Orr, Summary of workshop on dissolved organic carbon in the ocean, in *The Global Carbon Cycle*, edited by M. Heimann, pp. 584-585, Springer-Verlag, New York, 1993.

Yamanaka, Y., Development of ocean biogeochemical general circulation model, Ph.D. thesis, 90 pp., Univ. of Tokyo, Tokyo, 1995.

Yamanaka Y., and E. Tajika, The role of the vertical fluxes of particulate organic matter and calcite in the oceanic carbon cycle: Studies using an ocean biogeochemical general circulation model, *Global Biogeochem. Cycles*, *10*, 361-382, 1996.

E. Tajika, Geological Institute, School of Science, University of Tokyo, Bunkyo-ku, Tokyo, 113, Japan. (e-mail: tajika@geol.s.u-tokyo.ac.jp)

Y. Yamanaka, AOS Program, Sayre Hall, Princeton University, Princeton, NJ 08544. (e-mail: galapen@splash.princeton.edu)

(Received January 14, 1997; revised June 27, 1997; accepted July 30, 1997.)